

In vitro studies of lanthanide complexes for the treatment of osteoporosis†

Cite this: *Dalton Trans.*, 2013, **42**, 5999Yasmin Mawani,^a Jacqueline F. Cawthray,^a Stanley Chang,^a Kristina Sachs-Barrable,^b David M. Weekes,^a Kishor M. Wasan^{*b} and Chris Orvig^{*a}

Lanthanide ions, Ln(III), are of interest in the treatment of bone density disorders because they are found to accumulate preferentially in bone (*in vivo*), have a stimulatory effect on bone formation, and exhibit an inhibitory effect on bone degradation (*in vitro*), altering the homeostasis of the bone cycle. In an effort to develop an orally active lanthanide drug, a series of 3-hydroxy-4-pyridinone ligands were synthesized and eight of these ligands (H1 = 3-hydroxy-2-methyl-1-(2-hydroxyethyl)-4-pyridinone, H2 = 3-hydroxy-2-methyl-1-(3-hydroxypropyl)-4-pyridinone, H3 = 3-hydroxy-2-methyl-1-(4-hydroxybutyl)-4-pyridinone, H4 = 3-hydroxy-2-methyl-1-(2-hydroxypropyl)-4-pyridinone, H5 = 3-hydroxy-2-methyl-1-(1-hydroxy-3-methylbutan-2-yl)-4-pyridinone, H6 = 3-hydroxy-2-methyl-1-(1-hydroxybutan-2-yl)-4-pyridinone, H7 = 1-carboxymethyl-3-hydroxy-2-methyl-4-pyridinone, H8 = 1-carboxyethyl-3-hydroxy-2-methyl-4-pyridinone) were coordinated to Ln³⁺ (Ln = La, Eu, Gd, Lu) forming stable *tris*-ligand complexes (LnL₃, L = 1⁻, 2⁻, 3⁻, 4⁻, 5⁻, 6⁻, 7⁻ and 8⁻). The dissociation (pK_{an}) and metal ligand stability constants (log β_n) of the 3-hydroxy-4-pyridinones with La³⁺ and Gd³⁺ were determined by potentiometric titrations, which demonstrated that the 3-hydroxy-4-pyridinones form stable *tris*-ligand complexes with the lanthanide ions. One phosphinate-EDTA derivative (H₅XT = bis[[bis(carboxymethyl)amino]methyl]phosphinate) was also synthesized and coordinated to Ln³⁺ (Ln = La, Eu, Lu), forming the potassium salt of [Ln(XT)]²⁻. Cytotoxicity assays were carried out in MG-63 cells; all the ligands and metal complexes tested were observed to be non-toxic to this cell line. Studies to investigate the toxicity, cellular uptake and apparent permeability (P_{app}) of the lanthanide ions were conducted in Caco-2 cells where it was observed that [La(XT)]²⁻ had the greatest cell uptake. Binding affinities of free lanthanide ions (Ln = La, Gd and Lu), metal complexes and free 3-hydroxy-4-pyridinones with the bone mineral hydroxyapatite (HAP) are high, as well as moderate to strong for the free ligand with the bone mineral depending on the functional group.

Received 7th October 2012,
Accepted 12th December 2012

DOI: 10.1039/c2dt32373g

www.rsc.org/dalton

Introduction

Osteoporosis, the most prevalent bone density disorder, is a skeletal disease that is characterized by low bone mineral mass and a deterioration of bone tissue. Caused by an imbalance between bone formation and resorption, it leads to an increase in bone fragility and susceptibility of fracture. Often known as a “silent” disease because it is asymptomatic until

fracture occurs, it affects 200 million worldwide, putting an escalating pressure on health care resources.^{1,2} Primarily composed of osseous tissue, bone is responsible for structural support, protection of organs and storage of minerals in the body. Bone is a dynamic tissue that constantly undergoes resorption and desorption by a tightly regulated cycle in which it is destroyed by osteoclast cells and regenerated by osteoblast cells, as seen in Fig. 1.³ At the cellular level in osteoporotic bone, bone loss occurs because of a perturbation between the activity of osteoclasts and osteoblasts.^{4,5}

The most widely used class of drugs for the treatment of osteoporosis, bisphosphonates, are stable analogues of pyrophosphates that have a strong affinity for bone apatite; these agents inhibit bone resorption by reducing the recruitment and activity of osteoclasts and increasing apoptosis.^{6,7} Due to their poor lipophilicity, they possess very low oral bioavailability, typically <1%. As a result, bisphosphonates must be administered in a very high dosage to compensate for low

^aMedicinal Inorganic Chemistry Group, Department of Chemistry, University of British Columbia, 2036 Main Mall, Vancouver, British Columbia, Canada V6T 1Z1. E-mail: orvig@chem.ubc.ca

^bFaculty of Pharmaceutical Sciences, University of British Columbia, 2146 East Mall, Vancouver, BC, Canada V6T 1Z3. E-mail: kwasan@interchange.ubc.ca

†Electronic supplementary information (ESI) available: Detailed experimental procedures, ligand and metal complex characterization (Tables S.1–S.3), EC₅₀ data (Tables S.4–S.5), stepwise acid dissociation equilibria (Fig. S.1), speciation diagrams for metal complexes (Fig. S.2–S.3) and hydroxyapatite colourimetric assay (Fig. S.4). See DOI: 10.1039/c2dt32373g

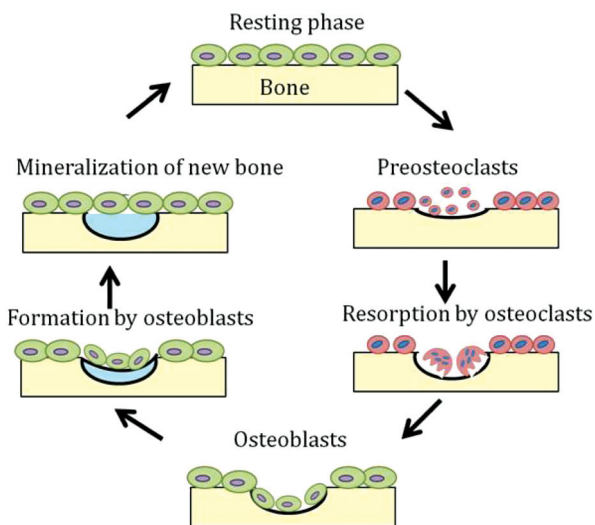


Fig. 1 Bone turnover cycle.^{5,16}

bioavailability, resulting in GI upset^{7,8} and low patient compliance.^{9,10} Additionally, there is mounting evidence indicating that bisphosphonates cause osteonecrosis of the jaw, with 5% of all cases associated with oral bisphosphonates used to treat osteoporosis.^{11–13} Likewise studies in dogs indicated that increased bone mineralization due to bisphosphonates leads to an inability to repair microcracks and microdamage, resulting in more fragile bone.^{12,14,15}

Due to the limitations of current therapies, our work¹⁷ has focused on the development of 3-hydroxy-4-pyridones and pyridinone lanthanide complexes for the treatment of osteoporosis. Lanthanide ions, which include the 14 4f-block elements as well as lanthanum, abbreviated herein as Ln(III), are isomorphous replacements of Ca(II) ions,^{18,19} sharing similar ionic radii, donor atom preferences, and almost identical coordination numbers in protein binding sites;²⁰ therefore, Ln(III) can potentially replace Ca(II) in bone, thus affecting the bone remodeling cycle.

For decades it has been known that lanthanide ions have a high affinity for bone,²¹ and it has been demonstrated that they can have an inhibitory effect on osteoclasts²² and a proliferative effect on osteoblasts.²³ Biodistribution studies in rats have shown that the heavier Ln(III) ions preferentially accumulate in bone rather than the liver or kidney, with 50–70% depositing in bone, compared to less than 25% for the lighter Ln.^{21,24} The elimination of Ln³⁺ from the bone is also slow, with a half life of 2.5 years; elimination from soft tissues such as the liver has a half life of about 15 days.^{21,24} A lanthanum carbonate preparation, Fosrenol (La₂(CO₃)₃), is a commercial agent for treatment of hyperphosphatemia, and also inhibits osteoclast activity while stimulating osteoblast proliferation.²⁵ However, pharmacokinetic studies in animals have shown that 94–99% of the administered lanthanum carbonate passed completely through the GI tract.²⁶ This strong elimination requires that high levels of the compound be administered, an undesirable protocol for chronic use, and suggests that

judicious ligand choice ought to positively influence biodistribution towards a modest uptake.

Thus adjustments to the ligand structure have potential to increase the oral bioavailability of the lanthanide ions. A library of 3-hydroxy-4-pyridinones and one phosphinate-EDTA ligand have been synthesized and complexed to lanthanide ions (Ln = La, Eu, Gd, Lu) under the principle of producing an orally active anti-osteoporotic agent that can pass through the gastrointestinal (GI) tract and effectively deliver lanthanides to bone.

Our previous studies focused on adjusting the ligand structure around Ln³⁺ (Ln = La, Eu, Tb, Yb) ions in order to increase the oral bioavailability of lanthanides, so as to decrease unwanted side effects.¹⁷ The suitability of these first generation lanthanide complexes for the treatment of bone resorption disorders was investigated in cellular uptake studies and bidirectional transport assays in Caco-2 cells, a model of the gastrointestinal (GI) lining. From these preliminary investigations it was found that one ligand HL1 (3-hydroxy-1,2-dimethyl-4-pyridinone) increased the lanthanide uptake into cells. The complexed form, La(L1)₃ (tris(1,2-dimethyl-3-hydroxy-4-pyridinonato)lanthanum(III)), was found to have low toxicity *in vitro*, and to have improved Caco-2 cell uptake compared to other compounds investigated, including lanthanum carbonate.¹⁷ One of the shortfalls of La(L1)₃ is its limited solubility in aqueous media, making it difficult to administer in *in vitro* and *in vivo* assays.

Optimizing the lipophilic/hydrophilic balance of the 3-hydroxy-4-pyridinones by varying the R₁-group (Fig. 2) has the potential to lead to further improvements in the GI uptake of the lanthanides. As the binding affinity of the ligand varies

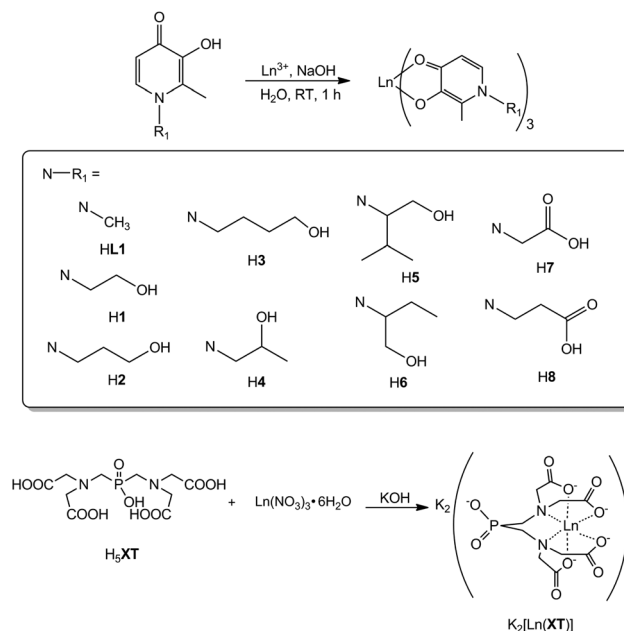


Fig. 2 A summary of the ligands and metal complexes, and their syntheses in this study; Ln = La, Eu, Gd and Lu.

minimally with changes to the R group, the hydrophilicity–lipophilicity balance can be tailored, with small or negligible changes in their chelating properties, to optimize this property for delivery to the sites where the ligand is required.^{27–30} These functional groups were carefully selected in order to tune the lipophilicity of the ligands, help direct the lanthanides towards bone, and to increase the water solubility of the complexes. Hydroxyl and carboxylate groups were selected because of their tendency to form hydrogen bonds and thus increase the water solubility of the ligands and their complexes; hydroxyl groups have also been shown to increase the affinity of complexes to bone.³¹ The alkyl chain length was varied to tune the lipophilicity of the ligands.²⁸

Additionally, one phosphinate-EDTA derivative (Fig. 2) was studied; this ligand was chosen to compare a hexadentate ligand system to that of the bidentate 3-hydroxy-4-pyridinone system. It was also selected due to the high affinity *in vivo* for phosphonate and phosphinate functional groups for bone.

Herein the synthesis of a library of 3-hydroxy-4-pyridinone complexes and one phosphinate-EDTA derivative and their respective lanthanide complexes are explored. The protonation constants of the free ligands and formation constants with La³⁺ and Gd³⁺ are also determined. The lipophilicity of the ligands, the toxicity of the ligands and complexes in MG-63 cells and Caco-2 cells are explored, along with the cell uptake and bifunctional transport in Caco-2 cells. Finally, the interaction of the metal complexes with hydroxyapatite (HAP) are discussed. A summary of the ligands and metal complexes can be seen in Fig. 2.

Results and discussion

Synthesis of 3-hydroxy-4-pyridinones

The syntheses of 3-hydroxy-2-methyl-4-pyridinones functionalized with carboxy and hydroxyl substituents were achieved by one of two routes – the direct ammonolysis of maltol, or the ammonolysis of benzyl-protected maltol, as seen in Scheme 1. The syntheses of H1 and H7 were accessed by the direct ammonolysis of the pyrone, maltol, with the appropriate

primary amine (Scheme 1, Route I). Generally, only the synthesis with small alkylamines can be achieved by the direct insertion method.²⁹ It is known that the insertion of the unprotected 3-hydroxy-4-pyrones leads to longer reaction times and difficulty isolating the product. As can be seen from Table S.1,† higher equivalents of the amine in the direct insertion syntheses were required to obtain yields comparable to the benzyl protected route.

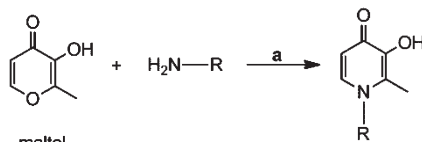
The syntheses of the remaining 3-hydroxy-4-pyridinones, H2, H3, H4, H5, H6, and H8, were prepared by a three step process (Scheme 1, Route II): first the 3-hydroxy functional group of the pyrone was protected with a benzyl-ether generating 3-benzyl-2-methyl-4-pyrene Bnma *via* a Williamson ether synthesis of maltol and benzylchloride.³² The Bnma was then reacted with the appropriate primary amine, affording Bn2, Bn3, Bn4, Bn5, Bn6, and Bn8, and finally the protecting group was removed to yield the free 3-hydroxy-2-methyl-4-pyridinones.

The syntheses of Bn2, B3 and Bn8 have been previously reported by Dobbin *et al.*³³ and were obtained in yields comparable to literature reports; Bn4 and Bn6 were all obtained in moderate yields. Bn6 required a higher equivalent of amine than did the other syntheses—this is mainly due to the steric hindrance of the nucleophile compared to the other amines, as can be seen in Table S.1.† Due to poor conversion rates from the pyrone to the pyridinone, the excess primary amine made separation of Bn5 from the starting materials difficult.

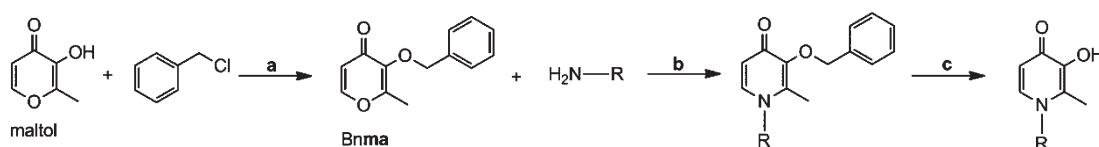
Once the key desired functional group was inserted into the pyridinone ring, the 3-benzoyloxy pyridinones could be deprotected to afford the free 3-hydroxy pyridinones, as shown in Scheme 1, Route II. Ligands H2, H3, H4, H5 and H6 were accessed by the palladium on carbon (P/C) catalyzed hydrogenation of Bn2, Bn3, Bn4, Bn5 and Bn6, respectively. For some of the ligands, in order to increase the aqueous solubility, a small amount of hydrochloric acid was added. Due to limited solubility of Bn8 in water, methanol or ethanol under neutral or acidic conditions, Bn8 was deprotected using HBr in glacial acetic acid.

The ligands were obtained in moderate to good yields, with the exception of H5. This is likely due to its poor solubility in

Route I:



Route II:



Scheme 1 General synthesis of a 3-hydroxy-4-pyridinone. Route I: (a) NaOH, H₂O, reflux 24–70 h. Route II: (a) benzyl chloride, NaOH, methanol, reflux 40 h; (b) NaOH, ethanol/water or methanol, reflux 15–92 h; (c) HBr in acetic acid 33% w/v or H₂(g), 10% P/C.

water and organic solvents. In the final step of the hydrogenation, the crude mixture must be filtered in order to remove the hydrogenation catalyst. Due to the limited solubility of H5, a significant amount of the ligand likely remained in the Pd–C mixture. Four literature 3-hydroxy-4-pyridinones were synthesized (H1, H2·HCl, H3·HCl and H8), along with three novel 3-benzyloxy-4-pyridinone ligands (H4, H5 and H6).

Synthesis and characterization of *tris*(pyridinonato)-lanthanide(III) complexes

All lanthanide pyridinone complexes were synthesized by the deprotonation of the 3-hydroxy of the pyridinone with sodium hydroxide in the presence a lanthanide(III) nitrate hexahydrate salt (Scheme 1). The complexes were synthesized in water, with the exception of La(5)₃; due to the limited solubility of H5 in water, La(5)₃ was synthesized in methanol. The ligands H1 and H7, were not soluble in water at room temperature, thus they were dissolved by the addition of NaOH; the pH was monitored so it was not above 4 to prevent hydrolysis of the metal ion. Once the ligand was dissolved, the desired lanthanide salt was added to the solution, and the pH was carefully adjusted to 9.5–10.5.

Complexation of the ligands was attempted with La³⁺, Eu³⁺, and Lu³⁺ and in most cases Gd³⁺, with the exception of H5 for which only the lanthanum complex was synthesized. The ¹H NMR spectra of the lanthanum and lutetium complexes were useful in elucidating the structure of the metal complexes. As seen in both Fig. 3 and Table S.2† the resonances for the ring hydrogens, H_a and H_b in the pyridinone metal complexes are shifted upfield compared to those of the free ligands. Similar upfield shifts have been previously reported in our lab.¹⁷ In the ¹H NMR spectra of the metal complexes, broad peaks were observed – this is attributed to the coordination of water in the coordination sphere, and to rapidly interconverting Δ and Λ stereoisomers and geometric *fac* and *mer* isomers at RT as well as both the Δ and Λ stereoisomers.³⁴

The IR spectra of all of the complexes were also helpful in confirming the formation of the complexes. Table S.3† gives a summary of the IR stretching frequencies of both the free ligands and the metal complexes, while IR spectra for H4 and

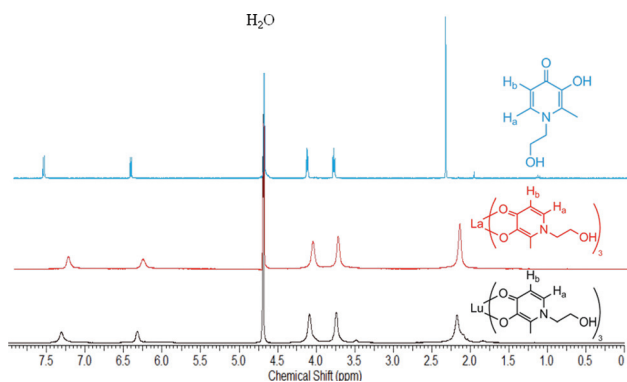


Fig. 3 ¹H NMR (400 MHz, D₂O, RT) spectra of H1 (top), La(1)₃ (middle) and Lu(1)₃ (bottom).

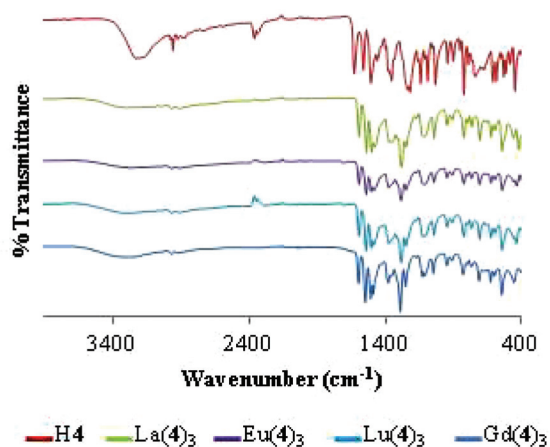


Fig. 4 Solid state IR spectra for, top to bottom: H4, La(4)₃, Eu(4)₃, Gd(4)₃ and Lu(4)₃; the spectra are offset for clarity.

the Ln(4)₃ complexes can be seen in Fig. 4. A characteristic four-band IR spectral pattern is observable at 1650–1460 cm⁻¹ in the free ligands; it can be attributed to the pyridinone ring and C=O stretching frequencies.^{35,36} Due to strong coupling, the ν_{ring} and $\nu_{\text{C=O}}$ stretching modes are indistinguishable from one another, thus the bands are collectively assigned to ν_{ring} and $\nu_{\text{C=O}}$ in Table S.3.† The metal complex spectra were dominated by peaks corresponding to the ligand (Fig. 4 and Table S.3†). Upon complexation, the characteristic four-band IR spectral pattern is preserved with a bathochromic shift around 30–50 cm⁻¹ and a possible reordering upon formation of the *tris*(3-oxy-4-pyridinonato)lanthanide complexes. When coordinated to a lanthanide ion, the $\nu_{\text{O-H}}$ stretch at 3300–3000 cm⁻¹ observed in the free ligand is replaced by a broad peak due to the coordination of waters in the lattice of the metal complex. The most distinctive characteristics upon complexation to a lanthanide ion are the new peaks between 400–550 cm⁻¹ assigned to the formation of metal–oxygen ($\nu_{\text{M-O}}$) stretching frequencies.³⁷ The IR spectra for the La³⁺, Eu³⁺, Gd³⁺ and Lu³⁺ complexes were all nearly superimposable within each ligand set, indicating that the metal complexes are isostructural. The <10 cm⁻¹ variation observed between the different metals is attributed to the size difference between the lanthanide ions. In the IR spectra of H8 and H9, very broad bands are observed around 3200 cm⁻¹, attributed to the strong intermolecular hydrogen bonding of the carboxyl groups.³⁸

Synthesis of a hexadentate phosphinate-EDTA derivative coordinated to lanthanide ions

Lanthanide ions were coordinated to H₅XT as previously reported by our laboratory.³⁹ K₂[Ln(XT)] was synthesized as the phosphinate functionality of the ligand could potentially help the complex localize towards bone, as in ¹⁵³Sm³⁺-EDTMP the bone seeking agent used in bone palliative care.^{40,41} Likewise, it was also synthesized so as to compare one hexadentate ligand *versus* three bidentate 3-hydroxy-4-pyridinones coordinated to the lanthanide ions.

Table 1 Acid dissociation constants (pK_{a1} , pK_{a2} , pK_{a3}) for the 3-hydroxy-4-pyridinone ligands HL1, H4 and H8 at 25 °C and 0.16 M NaCl. Numbers in parentheses represent SD between replicates

Constant	HL1	H4	H8
pK_{a1}^a	3.63(1)	3.11(3)	2.86(5)
pK_{a2}^a	9.71(1)	9.58(2)	3.99(4)
pK_{a3}^a			9.64(3)

^a Where $pK_{an} = -\log[K_{an}]$, $n = 1, 2, 3$.

Table 2 Log metal–ligand stability constants (β_n) and the ML_3OH metal–hydroxide stability constant ($\log K_4$) at 25 °C and 0.16 M NaCl. Numbers in parentheses represent SD between replicates

Constant	Equation	La ³⁺	Gd ³⁺
$\log \beta_1$	$M^{3+} + L^- \rightleftharpoons ML^{2+}$	7.06(5)	8.15(4)
$\log \beta_2$	$M^{3+} + 2L^- \rightleftharpoons ML_2^+$	12.6(1)	14.60(6)
$\log \beta_3$	$M^{3+} + 3L^- \rightleftharpoons ML_3$	17.5(1)	20.07(9)
$\log K_4$	$ML_3 + OH^- \rightleftharpoons ML_3(OH)^-$	7.94(6)	9.1(1)

Determination of stability constants of 3-hydroxy-4-pyridinones with lanthanide ions

The determination of the stability constants allows for the prediction of the thermodynamic stability of complexes *in vitro* and *in vivo* at physiologically relevant pHs. The two stepwise acid dissociation constants (pK_{an}) for HL1 and H4 (pK_{a1} and pK_{a2}) and the three stepwise acid dissociation constants for H8 (pK_{a1} , pK_{a2} and pK_{a3}), shown in Fig. S.1,† were determined for the amphoteric 3-hydroxy-4-pyridinones and are reported in Table 1.

The acid dissociation constants calculated for HL1 agree quite well with those reported previously in the literature.^{42–44} Likewise, the pK_{a2} of HL1 and H4 and the pK_{a3} of H8 are similar as seen in Table 1, indicating that the R group does not significantly alter the ionizability of the 3-hydroxyl group.³⁰ It also indicates that the deprotonated carboxethyl group of H8 does not significantly affect the electron density of the pyridinone ring.

The stability constants ($\log \beta_n$) of HL1 with La³⁺ and Gd³⁺ reported in Table 2 were determined using eqn (1) and (2). Not surprisingly, the binding constant of the ligand with Gd³⁺ is higher than that of La³⁺. This can easily be explained by the larger ionic radius of La³⁺ (103.2 pm, CN = 6)⁴⁵ versus that of Gd³⁺ (93.8 pm, CN = 6).⁴⁵ While the 3-hydroxy-4-pyridinones are known to form stable *tris*-ligand complexes with other trivalent cations such as Ga³⁺,⁴² In³⁺⁴² and Fe³⁺,^{43,44} the larger coordination sphere of the lanthanides, and their preferred coordination geometry of 8 or 9,⁴⁶ suggests the possibility of the formation of 4:1 complexes for HL1 with Ln³⁺ ions. As a result, excess of ligand was titrated in the presence of the lanthanides to achieve a 4:1 ligand to metal ratio but no

evidence of a 4:1 $[LnL_4]^-$ complex was observed with either La³⁺ or Gd³⁺ ions.

$$\beta_n = \frac{[ML_n^{(3-n)+}]}{[M^{3+}][L^-]^n} \quad (1)$$

$$K_4 = \frac{[ML_3(OH)^-]}{[ML_3][OH^-]} \quad (2)$$

Toxicity assay in MG-63 cells

MG-63 cells are derived from a human osteosarcoma⁴⁷ and were selected for cytotoxicity studies as they are considered to behave like osteoblasts.⁴⁸ Considering the vital role that osteoblasts play in the bone cycle (Fig. 1) and in the maintenance of bone mass, it is essential that compounds used for the potential treatment of osteoporosis are not toxic to MG-63 cells. A colourimetric MTT assay was utilized in order to quantify the toxicity of these compounds.⁴⁹ Cisplatin was used as a positive control to induce cell death, verifying the assay.

Cell viability was determined relative to the negative control, 100% cell medium, or 0.25% medium in DMSO. The half maximal effective concentration (EC_{50}) was calculated for cisplatin (Fig. 5a), confirming the assay was effective at determining toxicity; however, with the exception of La(2)₃, none of the synthesized ligands or Ln(III) complexes tested demonstrated any significant toxicity with the cell line at the concentrations tested. As a result, EC_{50} could not be calculated for the compounds tested. Tables S.4 and S.5† summarize the toxicities of the tested ligands and metal complexes in MG-63 cells, respectively. The low toxicity profiles ($EC_{50} > 100 \mu M$ for all tested ligands and complexes) of the synthesized compounds makes them of interest for the treatment of osteoporosis.

Partition coefficients

As the lipophilicity of a compound is such an important factor in drug screening,⁵⁰ the partition coefficients of the free ligands were determined by the shake-flask method.⁵¹ It should be noted that the lipophilicity of the free ligand (HL) compared to complexed ligand (Ln(L)₃) would likely be

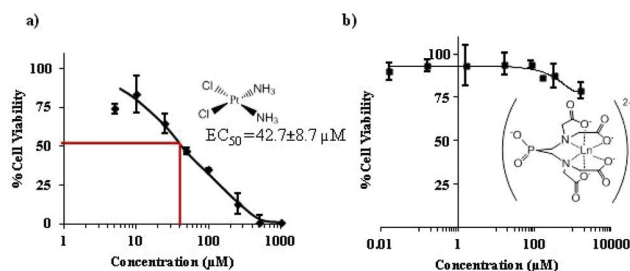


Fig. 5 Sample survival plots of MG-63 cells exposed to varying concentrations of compound for 48 h, monitored by the MTT assay, $n = 3$, error bars indicate \pm SD of the cell viability. The red line indicates the concentration at which 50% of the cells are no longer viable (EC_{50}); (a) cisplatin (positive control), (b) $[La(XT)]^{2-}$.

Table 3 Log $P_{o/w}$ coefficients of 3-hydroxy-4-pyridinones, in order of decreasing lipophilicities

Compound	Functional group (R_1)	Log $P_{o/w}$
H6	Secbutyl-OH	-0.42
H3	Butyl-OH	-0.76
HL1	Methyl	-0.77
H4	Isopropyl-OH	-0.82
H2	Propyl-OH	-0.86
H1	Ethyl-OH	-1.08
H8	Ethyl-carboxylate	-1.87
H7	Methyl-carboxylate	-1.95

markedly different; however, as only the R_1 group of the 3-hydroxy-4-pyridinones are varied, a quick screen was accomplished by the experimental determination of log $P_{o/w}$ of just the free ligands (eqn (3), Table 3).

$$\log P_{o/w} = \log \left(\frac{[\text{solute}]_{\text{octanol}}}{[\text{solute}]_{\text{water pH 7.4}}} \right) \quad (3)$$

There are two ligands, H6 and H3 with a log $P_{o/w}$ greater than that of HL1, the ligand from the first generation studies that when complexed to La^{3+} was found to have the greatest cell uptake and apparent permeability in Caco-2 cells;¹⁷ another two ligands, H4 and H2 have lipophilicities similar to that of HL1. Thus these ligands could potentially have similar or better cell uptake and apparent permeabilities than HL1.

Caco-2 cell studies

For the purposes of this study, first the toxicities of the compounds in Caco-2 cells were evaluated by an MTS assay.⁵² Triton-X 100 was used as a positive control to induce cell death. Much like the low toxicities observed for the metal complexes in the MG-63 cell line (Tables S.4 and S.5†), low cytotoxicity profiles were also observed in the Caco-2 cell line. EC_{50} values for $\text{La}(\mathbf{1})_3$, $\text{La}(\mathbf{2})_3$, $\text{La}(\mathbf{3})_3$, $\text{La}(\mathbf{4})_3$, $\text{La}(\mathbf{6})_3$, $\text{Na}_3[\text{La}(\mathbf{7})_3]$, $\text{Na}_3[\text{La}(\mathbf{8})_3]$ and $\text{K}_2[\text{La}(\mathbf{XT})]$ could not be calculated as all the compounds tested had >80% cell viability at a concentration of 1000 μM .

To evaluate the *in vitro* absorption of the lanthanide complexes, cell uptake and permeability studies in Caco-2 cell monolayers were carried out. As the GI tract remains the most acceptable route for the administration of drug formulations, it is important to evaluate if these drugs can cross the intestinal barriers. It has been demonstrated that Caco-2 cells, derived from a human colon adenocarcinoma,⁵³ have similar *in vitro* permeability characteristics as human intestinal tissue.⁵⁴ Under normal cell culture conditions, these epithelial cells spontaneously differentiate into enterocytes and form polarized monolayers.^{53,55} Several characteristics that mimic the small intestine are expressed; the Caco-2 cell monolayers possess well-developed brush border transport systems, enzymes, ion and nutrient channels.^{56,57} The cell monolayers have transepithelial electrical resistance (TEER) values of approximately 300 $\Omega \text{ cm}^{-2}$, similar to those found in the colon.⁵⁵ When cultured in transwell plates that contain a

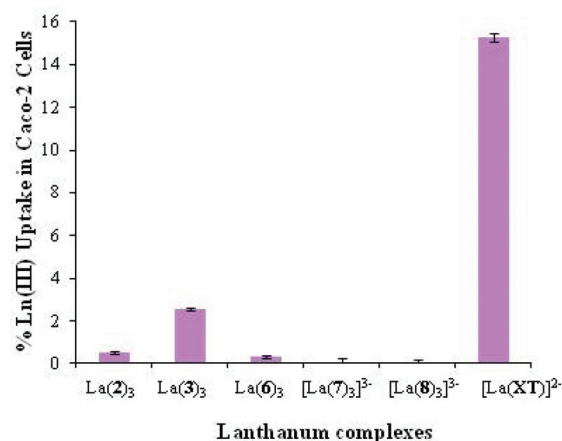


Fig. 6 Cell uptake of lanthanide complexes, $\text{La}(\mathbf{2})_3$, $\text{La}(\mathbf{3})_3$, $\text{La}(\mathbf{6})_3$, $[\text{La}(\mathbf{8})_3]^{3-}$, $[\text{La}(\mathbf{9})_3]^{3-}$ and $[\text{La}(\mathbf{XT})]^{2-}$ in Caco-2 cells, after 24 h exposure to compounds. Uptake data are reported as a mean percentage of the concentration of μM of Ln^{3+} taken up by the cells per mg of protein \pm SD, $n \geq 3$.

permeable membrane filter, the cells form distinct apical (top) and basolateral (bottom) membranes. It is the apical surface that possesses the brush border and transport systems that are characteristic of the small intestine, discussed above.⁵³ Thus Caco-2 cells, when plated in transwell plates, can be used to determine the *in vitro* transepithelial permeability coefficients or apparent permeability (P_{app}) of a drug. Several studies have demonstrated that the P_{app} ($A \rightarrow B$) across Caco-2 monolayers can be used to estimate the *in vivo* oral absorption of compounds.^{54,55,58}

In the Caco-2 cell uptake studies, as seen in Fig. 6, it was observed that one compound, $\text{K}_2[\text{La}(\mathbf{XT})]$ was found to have the greatest uptake. The uptake of $\text{K}_2[\text{La}(\mathbf{XT})]$ ($15.26 \pm 0.17\%$) is comparable to that determined for the lead compound from the first generation complexes, $\text{La}(\mathbf{1})_3$ ($9.07 \pm 2.33\%$).¹⁷ Moreover, $\text{K}_2[\text{La}(\mathbf{XT})]$ and $\text{La}(\mathbf{3})_3$ had greater cell uptake than did the benchmark $\text{La}_2(\text{CO}_3)_3$ compound, determined in previous studies.¹⁷ The lanthanide complexes, $\text{Na}_3[\text{La}(\mathbf{7})_3]$ and $\text{Na}_3[\text{La}(\mathbf{8})_3]$ had the poorest cell uptake, which correlated well with the log $P_{o/w}$ values determined for the ligands H7 and H8 (Fig. 6). The partition coefficients for H6 and H3 suggested that $\text{La}(\mathbf{6})_3$ would have better cell uptake than $\text{La}(\mathbf{3})_3$; however, as can be seen in Fig. 6, the opposite was found to be true.

It is theorized that the increased uptake of $[\text{La}(\mathbf{XT})]^{2-}$, compared to that of the lanthanide pyridinone complexes, has to do with the thermodynamic stability of the complex at physiological pH. A look at the speciation plot of $\text{La}(\mathbf{1})_3$ (Fig. S.2†), shows that at pH = 7.4 the complex is mainly in its 1:1 $\text{L}:\text{La}^{3+}$ and 2:1 $\text{L}:\text{La}^{3+}$ forms, with only a small amount in the 3:1 $\text{L}:\text{La}^{3+}$ form. Conversely, in the speciation plot³⁹ of $[\text{La}(\mathbf{XT})]^{2-}$ (Fig. S.3†) it is observed that at a pH of 7.4 the complex is intact. Thus, the increased stability of the $[\text{La}(\mathbf{XT})]^{2-}$ complex may result in more of the lanthanide being taken up by the cell, because the entire complex stays intact.

The $A \rightarrow B$ (apical to basolateral) transport in Caco-2 cells was also evaluated by introducing the lanthanide complexes to

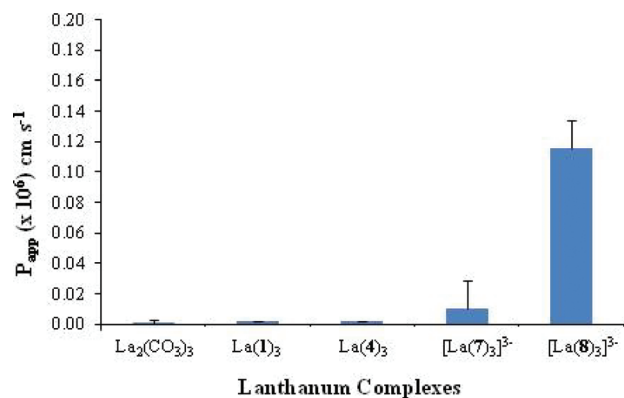


Fig. 7 Apparent permeability (P_{app}), apical to basolateral transport, of $\text{La}_2(\text{CO}_3)_3$, $\text{La}(\mathbf{1})_3$, $\text{La}(\mathbf{4})_3$, $[\text{La}(\mathbf{7})_3]^{3-}$ and $[\text{La}(\mathbf{8})_3]^{3-}$ in Caco-2 cells after 24 h of exposure to the lanthanide complexes reported as P_{app} $\text{cm s}^{-1} \pm \text{SD}$, $n \geq 3$.

the apical side of the cell monolayer in transwell plates. After an incubation time of 24 h, samples from the basolateral and apical side were analyzed for La^{3+} content by ICP-MS. The apparent permeability, P_{app} , was calculated by the determining the concentration of lanthanide in the basolateral side by ICP-MS at time point zero and at 24 h. The total lanthanide concentration added in the donor chamber (apical) was calculated by the addition of the amount of lanthanide content found in the apical, basolateral and cell lysate samples.

Apparent permeabilities were calculated for $[\text{La}(\mathbf{7})_3]^{3-}$, $[\text{La}(\mathbf{8})_3]^{3-}$, $\text{La}(\mathbf{1})_3$ and $\text{La}(\mathbf{4})_3$, and compared to $\text{La}_2(\text{CO}_3)_3$. The compound with the highest P_{app} value (Fig. 7) was found to be $\text{La}(\mathbf{4})_3$, which had $P_{app} = (0.12 \pm 0.02) \times 10^{-6}$ cm s^{-1} . The P_{app} of $\text{La}(\mathbf{4})_3$ was found to be an order of magnitude lower, compared to P_{app} calculated of the lead compound identified from the first generation complexes, $\text{La}(\mathbf{1})_3$.¹⁷ However, it should be noted that P_{app} of $\text{La}(\mathbf{4})_3$ was still found to be 700 times that of $\text{La}_2(\text{CO}_3)_3$, so a significant increase in bioavailability was achieved. Likewise, $\text{La}(\mathbf{4})_3$ has an apparent permeability three times that of the anti-osteoporotic drug alendronate.⁵⁹

Lanthanide complex binding studies with hydroxyapatite

Hydroxyapatite (HAP) was used as an *in vitro* model of bone; compounds were incubated under physiological conditions for different time points to evaluate the binding affinity of the Ln(III). ICP-MS was then used to measure the metal content in both the supernatant and the HAP pellet. As can be seen in Fig. 8, all the metals had near quantitative binding of the lanthanide to hydroxyapatite, with the exception of $\text{La}(\mathbf{4})_3$, with >98% to the HAP after 24 h. The high percentage of lanthanide bound correlates to our previous work.¹⁷ This indicates that the binding kinetics are quite fast, with >90% of the metal or metal–ligand complex bound to HAP after 5 minutes.

The lanthanide complexes, $\text{La}(\mathbf{4})_3$, $\text{Na}_3\text{Eu}(\mathbf{7})_3$, $\text{Na}_3\text{La}(\mathbf{8})_3$ and $\text{K}_2[\text{La}(\text{XT})]$ were all tested at very low concentration, 2 μM . This concentration was chosen firstly because it is well below the respective EC_{50} values which are reported in Table S.5,[†] meaning they are non-toxic at this concentration. Secondly, we wanted to ensure the amount that could interact with the HAP

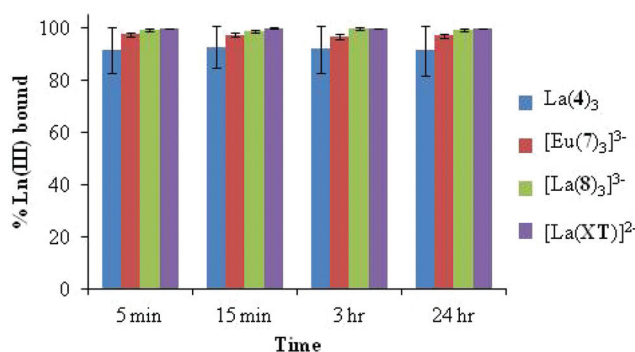


Fig. 8 Lanthanide metal complexes hydroxyapatite (HAP) binding studies analyzed by ICP-MS. Reported as the mean percentage \pm SD of Ln(III) bound to HAP, $n = 3$.

was greater than the amount seen to accumulate in bone in patients who are treated with lanthanum carbonate for 1 year.^{60,61}

While it is clear that the lanthanide ions are interacting with HAP, it is not clear if this is just a surface interaction, or if the Ln(III) is being incorporated into the HAP crystal lattice. Thus xylenol orange was used as an indicator for lanthanide binding. Xylenol orange is a colorimetric indicator of heavy metals,⁶² and is well known as an indicator for free lanthanides.^{63,64} In hexamethylenetetramine buffer, the ideal pH range for this heavy metal indicator is pH 4.5–6.0.⁶⁵

Under acidic conditions, xylenol orange is a deep red/purple colour when bound to free lanthanides. In contrast, unbound xylenol orange is a yellow-orange colour. Solutions of Ln-HAP supernatant, acid-digested Ln-HAP, undigested Ln-HAP, HAP (negative control), $\text{La}(\text{NO}_3)_3$ (positive control) were buffered to pH 5.0 and a solution of xylenol orange, buffered to pH 5.0 was introduced into each sample. As seen in Fig. S.4[†] the digested HAP is a deep red/purple, while the undigested HAP and supernatant samples are pale yellow; this assay confirms the ICP-MS results, showing a very small amount of free lanthanide in the supernatant from the undigested HAP sample. Likewise the absence of the deep red/purple colour in the undigested HAP sample, and the appearance of the red/purple upon digestion of the HAP indicates that the lanthanides are being incorporated into the HAP.

As it is clear that the lanthanides bind to HAP, and since these were much higher values (180 \times) compared to what was observed with the *in vivo* administration of $\text{La}_2(\text{CO}_3)_3$,^{60,61} it was important to study if the binding of lanthanides to the HAP caused structural or physical changes to the material. This assay was thus carried out on larger scale (0.5 g HAP vs. 20 mg of HAP) so there was enough to analyze HAP samples by TGA, PXRD, and FTIR.

As can be seen in Fig. 9a there is not a significant change in the FTIR of HAP with the metal or free ligand. The PXRD spectra shown in Fig. 9b also have no observable change; the peaks are all the same width and the d -spacing has not been altered by the addition of free ligand or the metal complex. Fig. 9c shows there is no change in the TGA—the small ($\sim 3\%$)

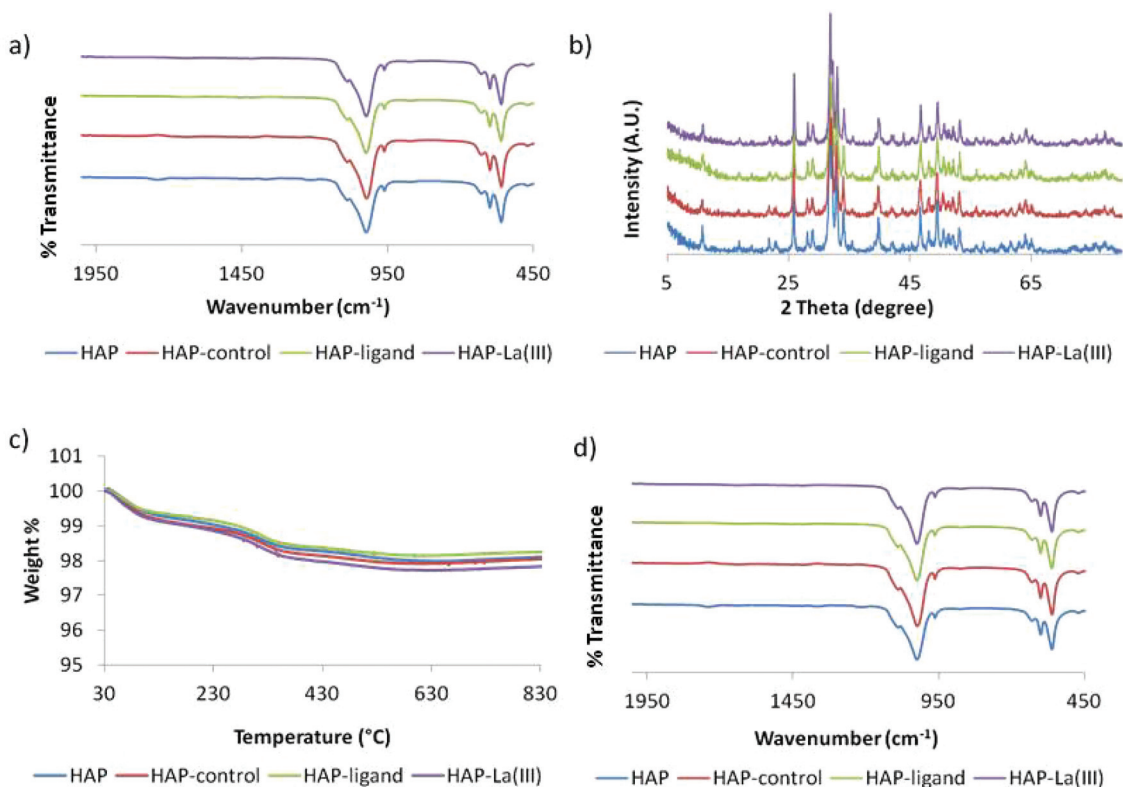


Fig. 9 Physical spectra of HAP sample (blue), HAP-control (red), HAP-free ligand (green) and HAP-metal (purple). Figure (a) FTIR of HAP samples before TGA, (b) XRD spectra of samples before TGA, (c) TGA of HAP samples and (d) FTIR of HAP samples after TGA. The FTIR and PXRD spectra are offset for clarity.

weight loss is likely due to the loss of 1 or 2 equivalents of water. Lastly Fig. 9d shows there is no change in the FTIR after the TGA when compared to the FTIR spectrum pre-TGA. With no observable change in the FTIR or the PXRD, it is obvious that the crystallinity of the HAP is not affected by the addition of the metal complex or free ligand.

Experimental

Materials

All solvents used for the synthesis of the ligands and metal complexes were HPLC grade and purchased from Fisher Scientific, as were anhydrous sodium sulphate, hydrochloric acid, potassium hydroxide, sodium chloride, sodium hydroxide and formaldehyde (aqueous solution 37% w/w), centrifuge tubes and Opitma nitric acid (a high purity acid containing the least metal content of any commercially available acid, used in trace metal analysis). Water was purified using an Elgastat Maxima HPLC reverse osmosis and deionization system or a PureLab Ultra system (Elga, Bucks, England). All water used was type 1, 18.2 MΩ cm, treated with a full spectrum UV to control bacterial levels. Maltol, 3-hydroxy-1,2-dimethyl-4-pyridinone (HL1, deferiprone), iminodiacetic acid and hypophosphorous acid (50% w/w aqueous solution) and La³⁺ and Gd³⁺ atomic absorption (AA) standards, hydroxyapatite, xylenol orange, 4-(2-hydroxyethyl)-1-piperazineethanesulfonic acid (HEPES) and 1-octanol

were purchased from Sigma-Aldrich, and the primary amines were purchased either from Sigma-Aldrich or Acros Organics. Lanthanum nitrate, europium nitrate, gadolinium nitrate and lutetium nitrate were purchased from Sigma-Aldrich and Alfa Aesar as their hexahydrates and used without further purification. Hydrobromic acid (33% w/v in glacial acetic acid) and sodium hydroxide solution (50%) were obtained from Acros Organics. For ICP-MS studies the lanthanide standards (1000 μg mL⁻¹ in 2% HNO₃) were purchased from High Purity Standards (North Charleston, SC, U.S.).

Both Caco-2 and MG-63 cells were obtained from American Type Culture Collection (ATCC, Rockville, MD, U.S.). Minimum essential media alpha (MEM-α), fetal bovine serum (FBS), 0.25% trypsin-EDTA, penicillin-streptomycin-neomycin 100× (Pen-Strep), phosphate buffer saline solution (PBS), Dulbecco's modified Eagle's medium (DMEM), fetal bovine serum (FBS), bovine serum albumin (BSA) and Hank's balanced salt solution (HBSS) were purchased from Life Technologies (Burlington, Ontario, Canada). T-75 culture flasks, transwell (12 well) and polycarbonate (12, 24 and 96-well) plates were purchased from Corning (Corning, NY, U.S.). Sterile 15 mL and 50 mL centrifuge tubes were purchased from Fisher Scientific. Barrier pipette tips were purchased from Diamed (Mississauga, Ontario, Canada). 3-(4,5-Dimethylthiazol-2-yl)-2,5-diphenyltetrazolium bromide (MTT) was purchased from Alfa Aesar and *cis*-diamminedichloroplatinum(II) (cisplatin) was obtained from Acros Organics. MTS Cell Titer 96® Aqueous One

Solution Cell Proliferation Assay and CytoTox96® Non-radioactive Cytotoxicity Assay were from Promega (Madison, WI, U.S.). Bicinchoninic acid assay (BCA) protein analysis kit was provided by Pierce (Rockford, IL, U.S.), while the lysis buffer, radioimmunoprecipitation assay (RIPA) was purchased from Sigma-Aldrich.

Instrumentation

Elemental analyses for C, H, and N were completed on a Fisons EA 1108 instrument while high resolution mass spectrometry (HRMS) electrospray ionization (ESI) was run on a Micromass LCT. Low resolution mass spectra (MS) were obtained on a Bruker Esquire Ion Trap ESI-MS spectrometer. ^1H and ^{13}C nuclear magnetic resonance (NMR) spectra were recorded at room temperature using a Bruker AV-300 or AV-400 spectrometer. Fourier transform infrared (FTIR) spectra were obtained on a Nicolet 6700 FTIR equipped with a Smart Orbit diamond attenuated total reflectance attachment. Lanthanide concentration was analyzed on a Perkin Elmer Sciex Elan 6000 inductively coupled plasma mass spectrometer (ICP-MS). Ultra-violet-visible (UV-vis) spectrum measurements were taken on a Varian Vary 100 Bio UV-vis. A Savant vacuum concentrator Speedvac Plus, model SC110A, was used at the highest temperature setting of 60 °C to concentrate the samples prior to acid digestion for ICP-analysis.

The absorbances of the plates for the MTT studies were measured at room temperature at 595 nm using a Beckman Coulter DTX 800 Multimode Detector. For the BCA and MTS assays the absorbances were measured at room temperature on a Multiskan Ascent Multi-plate reader from Labsystems at wavelengths of 492 nm and 540 nm, respectively. The trans-epithelial electrical resistance (TEER) values were monitored using a Millipore Millicell-ERS (Bedford, MA, U.S.). An Innova 44 incubator shaker (New Brunswick Scientific, Enfield, CT, U.S.) was used at 37 °C and 225 RPM to incubate the HAP samples. Ultra-violet-visible (UV-vis) spectrum measurements were acquired on a Varian Cary 100 Bio UV-Vis. A Fisher Scientific Minicentrifuge was used to separate HAP from supernatant and a Savant vacuum concentrator Speedvac Plus, model SC110A, was used at the highest temperature setting of 60 °C to concentrate HAP and supernatant samples prior to acid digestion for ICP-MS analysis. Powder X-ray diffraction samples were run on a Bruker AXS D8 Advance powder X-ray diffractometer, wavelength of $\text{CuK}\alpha$ (1.54 Å). For thermogravimetric analysis (TGA), samples were analyzed on a Perkin Elmer Pyris 6 thermogravimetric analyser.

Synthesis of ligands and metal complexes (Scheme 1)

3-Hydroxy-2-methyl-1-(2-hydroxyethyl)-4-pyridinone (H1)⁶⁶ and 1-carboxymethyl-3-hydroxy-2-methyl-4-pyridinone (H7)³⁸ were synthesized according to modified literature procedures. 3-Benzyloxy-2-methyl-4-pyrone (Bnma), synthesized according to our literature,³² was used to produce the intermediates 3-benzyloxy-2-methyl-1-(3-hydroxypropyl)-4-pyridinone hydrochloride (Bn2·HCl), 3-benzyloxy-2-methyl-1-(4-hydroxybutyl)-4-pyridinone hydrochloride (Bn3·HCl), 3-benzyloxy-2-methyl-

1-(2-hydroxypropyl)-4-pyridinone (Bn4), 3-benzyloxy-2-methyl-1-(1-hydroxy-3-methylbutan-2-yl)-4-pyridinone (Bn5), 3-benzyloxy-2-methyl-1-(1-hydroxybutan-2-yl)-4-pyridinone (Bn6) and 1-carboxyethyl-3-benzyloxy-2-methyl-4-pyridinone (Bn8). The synthesis of 3-hydroxy-2-methyl-1-(3-hydroxypropyl)-4-pyridinone hydrochloride (H2·HCl), 3-hydroxy-2-methyl-1-(4-hydroxybutyl)-4-pyridinone hydrochloride (H3·HCl), 3-hydroxy-2-methyl-1-(2-hydroxypropyl)-4-pyridinone (H4), 3-hydroxy-2-methyl-1-(1-hydroxy-3-methylbutan-2-yl)-4-pyridinone (H5), 3-hydroxy-2-methyl-1-(1-hydroxybutan-2-yl)-4-pyridinone (H6) and 1-carboxyethyl-3-hydroxy-2-methyl-4-pyridinone (H8) were synthesized by the deprotection of Bn2, Bn3, Bn4, Bn5, Bn6 and Bn8, according to a modification of literature.³³

General procedure for the synthesis of tris(pyridinonato) lanthanide complexes (Scheme 1)

The free 3-hydroxy-4-pyridinone (H1, H2, H3, H4, H5, H6, H7 or H8; 3.0 equiv.) was suspended in water or methanol (10 mL); $\text{Ln}(\text{NO}_3)_3 \cdot 6\text{H}_2\text{O}$ (1.0 equiv.) was added to the ligand solution and the pH of the mixture was raised slowly over 10–15 min with the dropwise addition of 1 M NaOH and the resulting mixture was continuously stirred for 1 h. The solution was concentrated under reduced pressure, redissolved in 1–2 mL of water and precipitated out with the addition of acetone (50 mL). The metal complex was collected by centrifugation (4000 RPM); the supernatant was discarded and the complex was dried *in vacuo*. The synthesis of bis[[bis(carboxymethyl)amino]methyl]-phosphinate ($\text{H}_5\text{XT}\cdot\text{HCl}$) and its respective metal complexes, $\text{K}_2[\text{Ln}(\text{XT})]$ were according to literature procedures.³⁹ Detailed synthetic procedures and characterization of all ligands and complexes can be found in the ESI.†

Potentiometric titrations

Potentiometric equilibrium measurements of the 3-hydroxy-4-pyridinones HL1, H4 and H9 and stability constant determinations of HL1 with La^{3+} and Gd^{3+} were performed on a Metrohm Titrand 809 equipped with a Ross combination pH electrode and a Metrohm Dosino 800 automatic burette. The titration apparatus consisted of a 10 mL water-jacketed glass vessel maintained at 25.0 ± 0.1 °C (Julabo water bath). Nitrogen, purified through a 10% NaOH solution to exclude any CO_2 , was passed through the solution prior and during the titrations. The electrode was calibrated using a standard HCl solution before each potentiometric equilibrium study. Data was collected in triplicate using PC Control (Version 6.0.91, Metrohm), and were analyzed by a standard computer treatment program (MacCalib) to obtain the calibration parameter E_0 .

A NaOH solution (0.15 M) was prepared from the dilution of 50% NaOH (Acros Organics) with freshly boiled 18.2 MΩ cm water under a stream of purified $\text{N}_2(\text{g})$, producing carbonate-free solution. The solution was standardized against freshly recrystallized potassium hydrogen phthalate. Titration of the NaOH solution with a standard HCl solution was performed regularly to determine the extent of carbonate accumulation in

the base solution and determined by plotting $(V_o + V_t) \times 10^{-\text{pH}}$ versus V_t (a Gran plot).⁶⁷

Determination of the acid dissociation constants was achieved by the titration of base into the ligand in acid. Ligand solutions (0.0010 M) were prepared by dissolving the ligands in a known amount of acid with an ionic strength of 0.16 M NaCl. Potentiometric titrations were performed by the automatic addition of base (CO₂ free NaOH) into the ligand solutions. While the equilibrium was rapidly established in less than 10 min, up to 15 min was permitted for stabilization between each addition of base.

The metal–ligand stability constants were obtained by the titration of base into variable ratio metal–ligand solutions, where the ligand concentration was kept constant and the concentration of either the La(III) or Gd(III) was varied. Metal ion solutions were prepared from the appropriate atomic absorption (AA) standard (Fluka, a subsidiary of Sigma-Aldrich). The exact amount of acid present in the metal standard was determined by titration of an equimolar solution of metal and Na₂H₂EDTA (disodium ethylenediaminetetraacetic acid), and determined from the corresponding Gran plot.⁶⁷ Metal ion solutions of La (0.00100–0.00029 M) and Gd (0.00100–0.00025 M) were prepared by dilution of the appropriate AA standard with HL1 (0.001 M) in a solution of 0.16 M NaCl. The ligand-to-metal ratios for the titrations were 1 : 1, 2 : 1, 3 : 1 and 4 : 1 for both HL1–La and HL1–Gd.

The hydrolysis constants for La(III)⁶⁸ and Gd(III)⁶⁹ were taken from Baes and Mesmer,⁶⁹ and Barnum⁶⁸ and were included in the calculations. The protonation constants of the ligands HL1, H4 and H9, and the metal–ligand stability constants with HL1 were calculated from the titration data using Hyperquad 2008.⁷⁰ All values and errors represent an average of at least three independent titration experiments.

MTT assay in MG-63 cells

The medium used to culture the MG-63 cells was minimum essential medium (MEM- α) supplemented with 10% fetal bovine serum (FBS) and 1% penicillin–streptomycin–neomycin 100X (Pen–Strep). The cells were incubated at 37 °C in a humidified atmosphere of 5% CO₂ and 95% O₂. Cells were cultured in T-75 cm³ Corning tissue culture flasks. Medium was changed every third day and every 5–6 days the cells were subcultured by trypsinization (0.5% trypsin-EDTA) to either new culture flasks or flat bottom 96-well plates. Cells were either passaged to new culture flasks, where 500 000 cells were cultured in each flask and incubated with 12 mL of medium, or to 96-well plates, where 10 000 cells were plated per well in 100 μL of medium.

Toxicity of the ligand and metal complexes was determined using a modified MTT (2-(4,5-dimethylthiazol-2-yl)-2,5-diphenyltetrazolium bromide) assay.⁴⁹ MG-63 cells were seeded into 96-well plates at a density of 10 000 cells per well in 100 μL of medium. After 24 h of incubation, the medium was exchanged for solutions of either the free ligands or the lanthanide complexes, affording concentrations of 0.01, 0.1, 10, 50, 100, 200, 500 and 1000 $\mu\text{g mL}^{-1}$ of compound dissolved in medium.

To determine the toxicity of La(L1)₃, due to its limited aqueous solubility, a 0.25% DMSO/medium solution was used to test the complex; also as a result of limited solution, the highest concentration of La(L1)₃ tested was 600 $\mu\text{g mL}^{-1}$. As a positive control cisplatin (*cis*-diamminedichloroplatinum(II)) was incubated at concentrations of 1, 5, 10, 25, 50, 100, 250, 500 and 1000 μM in 0.25% DMSO/medium. As negative controls, 100% medium and 0.25% DMSO/medium were incubated with the cells. For each compound concentration, the assay was performed in triplicate.

After 48 h of treatment a 50 μL aliquot of MTT (2.5 mg mL⁻¹ in PBS) was added to each well of the plate. The cells were incubated for 3 h with the MTT solution, allowing for the formation of formazan crystals at the bottom of the wells. The MTT/media/compound treatment was aspirated, leaving the formazan crystals, which were subsequently dissolved in 100 μL of DMSO. The absorbance of each well was measured at 595 nm using a Beckman Coulter DTX 800 Multimode Detector. Cell viability was calculated relative to the negative control (representative of 100% cell viability). The EC₅₀ value was determined by finding the concentration at which 50% of the cells were viable, relative to the negative control.

Determination of the octanol–water partition coefficient ($P_{o/w}$)

The shake-flask method⁵¹ was used to determine the octanol–water partition coefficients of the free ligands, and were calculated according to eqn (3). A detailed experimental description can be found in the ESI.†

Caco-2 cell culture

Cells were cultured in complete Dulbecco's modified Eagle's medium (DMEM), supplemented with 10% fetal bovine solution (FBS), 292 $\mu\text{g mL}^{-1}$ L-glutamine, 0.1 mM non-essential amino acids, 100 $\mu\text{g mL}^{-1}$ penicillin and 100 $\mu\text{g mL}^{-1}$ streptomycin in T-75 flasks, 12-well transwell, 12-well, 24-well or 96-well plates depending on the type of experiment. Cells were incubated at 37 °C in a humidified atmosphere of 5% CO₂ and 95% O₂ and the medium was refreshed every other day. Cells were used for studies once they reached 80% confluency.

Caco-2 cell MTS assay

Toxicities of the ligand and metal complexes were determined using a modified MTS (3-(4,5-dimethylthiazol-2-yl)-5-(3-carboxymethoxyphenyl)-2-(4-sulfophenyl)-2H-tetrazolium) assay.⁵² Caco-2 cells were seeded onto 96-well plates at a density of 40 000 cells cm⁻² and the medium was refreshed every 48 h. When the cells reached 80% confluency, they were washed 3 times with Hanks balanced salt solution (HBSS) and the culture medium was exchanged for treatment solutions up to 1000 μM for La(1)₃, La(2)₃, La(3)₃, La(4)₃, La(6)₃, Na₃[La(7)₃], Na₃[La(8)₃], K₂[La(XT)], 1% Triton X-100 (positive control) and media only (negative control). For each compound concentration, the assay was performed in triplicate. After the cells were incubated for 24 h with the lanthanide complexes, MTS (Cell Titer 96R Aqueous One Solution Cell Proliferation Assay Kit) was added to each well. The plate was wrapped in aluminium foil

and incubated for 3–4 h at 37 °C in a humidified atmosphere of 5% CO₂ and 95% O₂, allowing for the formation of soluble formazan crystals. Absorbance was measured at room temperature at 492 nm with a Multiskan Ascent Multi-plate reader from Labsystems. Cell viability was calculated relative to the negative control (representative of 100% cell viability). The EC₅₀ value was determined by finding the concentration at which 50% of the cells were viable, relative to the negative control.

Caco-2 cell protein concentration assay

After performing the cell uptake and bifunctional transport assays, cells were lysed (*vide infra*), and protein concentrations of the cell lysates were measured by a bicinchoninic acid protein assay (BCA Protein Assay Kit).⁷¹ A procedure modified from that reported previously by our group was used to study the protein concentrations.¹⁷ For a detailed experimental description, please see the ESI.†

Caco-2 cell uptake studies

Caco-2 cells were seeded at 10 000 cells cm⁻² in 12 or 24-well plates and the medium was refreshed every other day until 80–90% confluency was reached. On the day of the experiment, the cells were washed 3 times with PBS and the culture medium was exchanged for treatment solutions of La(2)₃, La(3)₃, La(6)₃, Na₃[La(7)₃], Na₃[La(8)₃], K₂[La(XT)] or medium (negative control) at concentrations up to 1000 μM. The cells were then incubated with the compounds for 24 h. Treatment solutions were aspirated and the cells were washed three times with PBS. After wrapping the plates in aluminium foil, they were stored at –20 °C until analysis. Cells were lysed with 250 μL of lysis buffer (RIPA); the cell lysate solutions from each well were transferred into separate 2 mL Eppendorf tubes. The wells were rinsed with another 250 μL of lysis buffer (RIPA); 60–75 μL from each sample was removed for protein analysis by a Pierce BCA assay to determine protein concentration. The remaining 425–440 μL were reserved later for La³⁺ analysis by ICP-MS. The concentrations are reported as % uptake of La³⁺ ion (μM)/mg of protein/well ± SD.

Caco-2 cell permeability studies

Caco-2 cells were seeded at 5000 cells cm⁻² in polycarbonate membrane 12-well transwell plates. The medium was exchanged every other day and uptake studies were conducted when TEER readings reached 500 Ω cm⁻². Prior to the addition of the lanthanide compounds, the culture medium was removed, washed with PBS and replaced with fresh medium in the basolateral (bottom) chamber and fresh medium (negative control), or medium plus compound (treatment), with concentrations up to 1000 μM in the apical (top) chamber. After 24 h incubation, the integrity of the Caco-2 cell monolayers was monitored by measuring the TEER value; 0.3–0.4 mL of medium from the apical chamber and 1 mL from the basolateral chamber were retained for analysis of lanthanide ion content by ICP-MS. The cells were washed three times with PBS, and the polycarbonate membranes were removed, lysed

in 250 μL of lysis buffer (RIPA) and transferred into a 2 mL Eppendorf tubes. The wells were rinsed with another 250 μL of lysis buffer (RIPA) and collected in the same Eppendorf tubes; 60–75 μL from each sample was removed for protein analysis by a Pierce BCA assay to determine the protein concentration. The remaining 425–400 μL were reserved for later La³⁺ analysis by ICP-MS. The concentration of Ln³⁺ accumulated in the cells, and the apical and basolateral chambers were evaluated by ICP-MS.

The apparent permeability (P_{app} , cm s⁻¹) coefficients from the bidirectional transport of the Ln³⁺ complexes were calculated using eqn (4). $\Delta Q/\Delta t$ (nmol s⁻¹) was the flow rate for mass transport across monolayers, A was the surface area of the insert membrane (1.13 cm²), and C₀ was the initial concentration (μM) of the compound added in the apical chamber. The flow rate was calculated by plotting the rate (nmol) of compound increase as a function of time (s) in the donor (basolateral) chamber.

$$P_{app} = \frac{(\Delta Q/\Delta t)}{(A \cdot C_0)} \quad (4)$$

Lanthanum ion analysis by ICP-MS

All materials used for the acid digestion process were soaked in a 5% Extran bath overnight, rinsed with 18.2 MΩ cm water, and washed in a 1% Optima nitric acid bath overnight. Materials were then washed with 18.2 MΩ cm water and left to dry in a dust free environment overnight. A lanthanide calibration curve for ICP-MS analysis was prepared by serial dilutions of the lanthanum standard (1000 μg mL⁻¹) in 1% Optima nitric acid, and analyzed at concentrations ranging from 0.0001–10 ppm, where 1 part per million (ppm) is equivalent to 1 μg mL⁻¹. The count number was then plotted *versus* the concentration of the lanthanum ion in ppm. Concentration of lanthanide in each sample was then determined against the standard calibration curve.

Acid digestion for ICP-MS analysis

The samples were dissolved in 2 mL of concentrated Optima nitric acid and transferred into test tubes (16 × 150 mm) with 1–2 Teflon boiling chips and placed in a block heater. The temperature was raised to 105 °C and maintained overnight. The solutions were cooled to room temperature and 2 mL of 30% hydrogen peroxide was added to each sample which was then heated to 140 °C overnight. The temperature was increased to 150–160 °C until samples were evaporated to dryness. Samples were then dissolved in exactly 3.00 mL of 10% Optima nitric acid in water (% v/v) and stored in 15 mL centrifuge tubes at 4 °C until analysis for metal ion content.

Hydroxyapatite *in vitro* binding study

A procedure modified from that reported previously by our group was used to study the *in vitro* hydroxyapatite binding of the metal complexes.¹⁷ For a detailed experimental description, please see the ESI.†

Analysis by xylenol orange assay

A procedure modified from that reported previously by our group was used to qualitatively analyze the *in vitro* hydroxyapatite binding of the metal complexes.¹⁷ For a detailed experimental description, please see the ESI.†

Conclusions

A series of 3-hydroxy-4-pyridinone ligands were successfully synthesized. The 3-hydroxy-4-pyridinones were rationally designed to incorporate a number of different functional groups that possess varying lipophilicities and low toxicity profiles. The alcohol and carboxy derivatized 3-hydroxy-4-pyridinone ligands were coordinated to a variety of lanthanides ($\text{Ln}^{3+} = \text{La}, \text{Eu}, \text{Gd}, \text{Lu}$). Three ligands (H4, H9 and HL1) were studied for their acid dissociation constants (pK_a), all possessing similar pK_a s for the 3-hydroxy hydrogen. The stability constants were determined for one ligand, HL1, with La^{3+} and Gd^{3+} , confirming the formation of stable tris-ligand complexes with 3-hydroxy-4-pyridinones. The metal complexes proved to possess low cytotoxicity profiles in MG-63 cells ($\text{EC}_{50} > 100 \mu\text{M}$), and a high affinity for HAP (>90%). The most promising 3-hydroxy-4-pyridinone complex in this study, $\text{La}(\mathbf{4})_3$, was 700 times more bioavailable than $\text{La}_2(\text{CO}_3)_3$ as determined by the apparent permeabilities of the compounds in Caco-2 cells, an assay that mimics the absorption of compounds across the GI tract.

One phosphinate-EDTA ligand (H_5XT) was synthesized, and coordinated to lanthanide ions ($\text{Ln}^{3+} = \text{La}, \text{Eu}, \text{Lu}$). $[\text{La}(\text{XT})]^{2-}$ as its potassium salt proved to have the greatest uptake in Caco-2 cells, and was clearly identified as the lead compound from these studies. The cell uptake of $[\text{La}(\text{XT})]^{2-}$ ($15.26 \pm 0.17\%$) in Caco-2 cells was found to be higher than $\text{La}(\mathbf{L1})_3$ ($9 \pm 2\%$), the lead compound identified from the first generation studies.¹⁷ Likewise the low toxicity of $[\text{La}(\text{XT})]^{2-}$ and the high binding affinity for HAP (>98% after 24 h) warrants further investigation of this complex. Moreover, the low toxicity profile of both $[\text{Eu}(\text{XT})]^{2-}$ and $[\text{Lu}(\text{XT})]^{2-}$ in MG-63 cells also justifies further investigation into the entire series of lanthanide ions coordinated by H_5XT .

Acknowledgements

We thank Dr Elena Polishchuk and Jessie Chen for help and knowledge about cells, Vivian W.-M. Lai and Dr Robin Stoodley for their expertise with ICP-MS and Dr Rizhi Wang for his expertise on hydroxyapatite and providing MG-63 cells. We also acknowledge support of the Natural Sciences and Engineering Research Council of Canada (NSERC) and the Canadian Institutes of Health Research (CHIR) for their Collaborative Health Research Projects (CHRP) funding. C.O. acknowledges the Canada Council for the Arts for a Killam Research Fellowship (2011–2013).

References

- Osteoporosis. *Government of Canada* (Accessed: May 23, 2012, <http://www.biobasics.gc.ca/english/view.asp?x=770>).
- J.-Y. Reginster and N. Burlet, *Bone*, 2006, **38**, 4–9.
- P. V. Hauschka, A. E. Mavrakos, M. D. Iafrazi, S. E. Doleman and M. Klagsbrun, *J. Biol. Chem.*, 1986, **261**, 2665–2674.
- L. G. Raisz, *Clin. Chem.*, 1999, **45**, 1353–1358.
- P. Sambrook, in *Primer on the Rheumatic Diseases*, ed. J. H. Klippel, J. H. Stone, L. J. Crofford and P. H. White, Springer, New York, 2008, pp. 584–591.
- H. Skarpos, S. N. Osipov, D. V. Vorob'eva, I. L. Odinets, E. Lork and G. V. Rosenthaler, *Org. Biomol. Chem.*, 2007, **5**, 2361–2367.
- E. Guenin, M. Monteil, N. Bouchemal, T. Prange and M. Lecouvey, *Eur. J. Org. Chem.*, 2007, 3380–3391.
- A. Hoffman, D. Stepensky, A. Ezra, J. M. Van Gelder and G. Golomb, *Int. J. Pharm.*, 2001, **220**, 1–11.
- J. A. Cramer, M. M. Amonkar, A. Hebborn and R. Altman, *Curr. Med. Res. Opin.*, 2005, **21**, 1453–1460.
- J. A. Cramer, D. T. Gold, S. L. Silverman and E. M. Lewiecki, *Osteoporosis Int.*, 2007, **18**, 1023–1031.
- S. Khosla, D. Burr, J. Cauley, D. W. Dempster, P. R. Ebeling, D. Felsenberg, R. F. Gagel, V. Gilsanz, T. Guise, S. Koka, L. K. McCauley, J. McGowan, M. D. McKee, S. Mohla, D. G. Pendrys, L. G. Raisz, S. L. Ruggiero, D. M. Shafer, L. Shum, S. L. Silverman, C. H. Van Poznak, N. Watts, S.-B. Woo and E. Shane, *J. Bone Miner. Res.*, 2007, **22**, 1479–1491.
- D. B. Burr, L. Miller, M. Grynepas, J. L. Li, A. Boyde, T. Mashiba, T. Hirano and C. C. Johnston, *Bone*, 2003, **33**, 960–969.
- P. J. Meunier and G. Boivin, *Bone*, 1997, **21**, 373–377.
- T. Mashiba, C. H. Turner, T. Hirano, M. R. Forwood, C. C. Johnston and D. B. Burr, *Bone*, 2001, **28**, 524–531.
- C. H. Turner, *Osteoporosis Int.*, 2002, **13**, 97–104.
- D. J. Hadjidakis and I. I. Androulakis, in *Women's Health and Disease: Gynecologic, Endocrine, and Reproductive Issues*, ed. G. Creatas, G. Mastorakos and G. P. Chrousos, Wiley-Blackwell, Hoboken, 2006, vol. 1092, pp. 385–396.
- C. A. Barta, K. Sachs-Barrable, J. Jia, K. H. Thompson, K. M. Wasan and C. Orvig, *Dalton Trans.*, 2007, 5019–5030.
- S. P. Fricker, *Chem. Soc. Rev.*, 2006, **35**, 524–533.
- C. H. Evans, *Trends Biochem. Sci.*, 1983, **8**, 445–449.
- E. R. Birnbaum, J. E. Gomez and D. W. Darnall, *J. Am. Chem. Soc.*, 1970, **92**, 5287–5288.
- P. W. Durbin, M. H. Williams, M. Gee, R. H. Newman and J. G. Hamilton, *Proc. Soc. Exp. Biol. Med.*, 1956, **91**, 78–85.
- J. C. Zhang, S. J. Xu, K. Wang and S. F. Yu, *Chin. Sci. Bull.*, 2003, **48**, 2170–2175.
- J. Zhang, C. Liu, Y. Li, J. Sun, P. Wang, K. Di and Y. Zhao, *J. Rare Earths*, 2010, **28**, 138–142.
- T. J. Haley, in *Handbook on the Physics and Chemistry of Rare Earths*, ed. J. K. A. Gschneider and L. Eyring, North-Holland, Amsterdam, 1979, vol. 4, pp. 553–585.

- 25 N. D. Atherton, J. W. Totten and M. D. Gaitonde, *Treatment of Bone Disorders, U.S. Pat.*, 7,078,059, Jul 18, 2006.
- 26 S. J. P. Damment and I. Webster, *J. Am. Soc. Nephrol.*, 2003, **14**, 204A–205A.
- 27 J. Burgess, M. Rangel and E. Rudi van, in *Advances in Inorganic Chemistry*, Academic, 2008, vol. 60, pp. 167–243.
- 28 M. A. Santos, M. Gil, L. Gano and S. Chaves, *J. Biol. Inorg. Chem.*, 2005, **10**, 564–580.
- 29 C. Queiros, M. J. Amorim, A. Leite, M. Ferreira, P. Gameiro, B. de Castro, K. Biernacki, A. Magalhaes, J. Burgess and M. Rangel, *Eur. J. Inorg. Chem.*, 2011, 131–140.
- 30 J. B. Porter, M. Gyparakis, L. C. Burke, E. R. Huehns, P. Sarpong, V. Saez and R. C. Hider, *Blood*, 1988, **72**, 1497–1503.
- 31 R. G. G. Russell, *Ann. N. Y. Acad. Sci.*, 2006, **1068**, 367–401.
- 32 W. O. Nelson, T. B. Karpishin, S. J. Rettig and C. Orvig, *Can. J. Chem.*, 1988, **66**, 123–131.
- 33 P. S. Dobbin, R. C. Hider, A. D. Hall, P. D. Taylor, P. Sarpong, J. B. Porter, G. Xiao and D. van der Helm, *J. Med. Chem.*, 1993, **36**, 2448–2458.
- 34 W. O. Nelson, T. B. Karpishin, S. J. Rettig and C. Orvig, *Inorg. Chem.*, 1988, **27**, 1045–1051.
- 35 A. R. Katritzky and R. A. Jones, *J. Chem. Soc.*, 1960, 2947–2953.
- 36 D. Cook, *Can. J. Chem.*, 1963, **41**, 2575–2584.
- 37 K. S. Mazdiyasi and L. M. Brown, *Inorg. Chem.*, 1970, **9**, 2783–2786.
- 38 Z. Zhang, S. J. Rettig and C. Orvig, *Can. J. Chem.*, 1992, **70**, 763–770.
- 39 L. Xu, S. J. Rettig and C. Orvig, *Inorg. Chem.*, 2001, **40**, 3734–3738.
- 40 P. Anderson, *Expert Opin. Pharmacother.*, 2006, **7**, 1475–1486.
- 41 O. G. Finlay, M. D. Mason and M. Shelley, *Lancet Oncol.*, 2005, **6**, 392–400.
- 42 D. J. Clevette, D. M. Lyster, W. O. Nelson, T. Rihela, G. A. Webb and C. Orvig, *Inorg. Chem.*, 1990, **29**, 667–672.
- 43 R. J. Motekaitis and A. E. Martell, *Inorg. Chim. Acta*, 1991, **183**, 71–80.
- 44 M. A. Kline and C. Orvig, *Clin. Chem.*, 1992, **38**, 562–565.
- 45 R. D. Shannon, *Acta Crystallogr., Sect. A: Cryst. Phys., Diffraction, Theor. Gen. Cryst.*, 1976, **32**, 751–767.
- 46 M. A. Jakupiec, P. Unfried and B. K. Keppler, *Rev. Physiol., Biochem., Pharmacol.*, 2005, **153**, 101–111.
- 47 Z. Xue, M. Lin, J. Zhu, J. Zhang, Y. Li and Z. Guo, *Chem. Commun.*, 2010, **46**, 1212–1214.
- 48 D. Lajeunesse, *Bone Miner.*, 1994, **24**, 1–16.
- 49 T. Mosmann, *J. Immunol. Methods*, 1983, **65**, 55–63.
- 50 C. A. Lipinski, *J. Pharmacol. Toxicol. Methods*, 2000, **44**, 235–249.
- 51 OECD, in *OECD Guidelines for the Testing of Chemicals, Section 1*, OECD Publishing, 1995, p. 1.
- 52 T. M. Buttke, J. A. McCubrey and T. C. Owen, *J. Immunol. Methods*, 1993, **157**, 233–240.
- 53 X.-P. Huang, M. Spino and J. Thiessen, *Pharm. Res.*, 2006, **23**, 280–290.
- 54 W. Rubas and M. E. M. Cromwell, *Adv. Drug Delivery Rev.*, 1997, **23**, 157–162.
- 55 P. Artursson and J. Karlsson, *Biochem. Biophys. Res. Commun.*, 1991, **175**, 880–885.
- 56 C.-Y. Huang, C.-Y. Lee, M.-Y. Chen, H.-C. Tsai, H.-C. Hsu and C.-H. Tang, *J. Cell. Physiol.*, 2010, **224**, 475–483.
- 57 Z. Yan, J. Sun, Y. Chang, Y. Liu, Q. Fu, Y. Xu, Y. Sun, X. Pu, Y. Zhang, Y. Jing, S. Yin, M. Zhu, Y. Wang and Z. He, *Mol. Pharm.*, 2011, **8**, 319–329.
- 58 M. Yazdaniyan, S. L. Glynn, J. L. Wright and A. Hawi, *Pharm. Res.*, 1998, **15**, 1490–1494.
- 59 A. Ezra, A. Hoffman, E. Breuer, I. S. Alferiev, J. Mönkkönen, N. El Hanany-Rozen, G. Weiss, D. Stepensky, I. Gati, H. Cohen, S. Törmälehto, G. L. Amidon and G. Golomb, *J. Med. Chem.*, 2000, **43**, 3641–3652.
- 60 P. C. D'Haese, G. B. Spasovski, A. Sikole, A. Hutchison, T. J. Freemont, S. Sulkova, C. Swanepoel, S. Pejanovic, L. Djukanovic, A. Balducci, G. Coen, W. Sulowicz, A. Ferreira, A. Torres, S. Curic, M. Popovic, N. Dimkovic and M. E. De Broe, *Kidney Int.*, 2003, **63**, S73–S78.
- 61 G. B. Spasovski, A. Sikole, S. Gelev, J. Masin-Spasovska, T. Freemont, I. Webster, M. Gill, C. Jones, M. E. De Broe and P. C. D'Haese, *Nephrol., Dial., Transplant.*, 2006, **21**, 2217–2224.
- 62 A. Hulanicki, S. Glab and G. Ackermann, *Pure Appl. Chem.*, 1983, **55**, 1137–1230.
- 63 M. Ali, M. Woods, E. Suh, Z. Kovacs, G. Tirsó, P. Zhao, V. Kodibagkar and A. Sherry, *J. Biol. Inorg. Chem.*, 2007, **12**, 855–865.
- 64 E. Gaidamauskas, H. Parker, B. A. Kashemirov, A. A. Holder, K. Saejueng, C. E. McKenna and D. C. Crans, *J. Inorg. Biochem.*, 2009, **103**, 1652–1657.
- 65 S. J. Lyle and M. M. Rahman, *Talanta*, 1963, **10**, 1177–1182.
- 66 N. A. Epstein, J. L. Horton, C. M. Vogels, N. J. Taylor and S. A. Westcott, *Aust. J. Chem.*, 2000, **53**, 687–691.
- 67 G. Gran, *Analyst*, 1952, **77**, 661–671.
- 68 D. W. Barnum, *Inorg. Chem.*, 1983, **22**, 2297–2305.
- 69 C. F. Baes and R. E. Mesmer, *The Hydrolysis of Cations*, Wiley, 1976.
- 70 P. Gans, A. Sabatini and A. Vacca, *Talanta*, 1996, **43**, 1739–1753.
- 71 J. M. Walker, in *The Protein Protocols Handbook*, ed. J. M. Walker, Humana, Totawa, 2nd edn, 2002, pp. 11–14.